EUMETSAT Satellite Application Facility on Climate Monitoring

Algorithm Theoretical Basis Document
SEVIRI cloud products
CLAAS Edition 2

DOI: 10.5676/EUM_SAF_CM/CLAAS/V002

Fractional Cloud Cover	**CM-21011**
Joint Cloud property histogram	**CM-21021**
Cloud Top level	**CM-21031**
Cloud Phase	**CM-21041**
Liquid Water Path	**CM-21051**
Ice Water Path	**CM-21061**

Reference Number:	SAF/CM/DWD/ATBD/SEV/CLD
Issue/Revision Index:	2.3
Date:	17.06.2016

Document Signature Table

	Name	Function	Signature	Date
Authors	Jan Fokke Meirink Martin Stengel	CM SAF scientist CM SAF scientist		21/04/2016
Editor	Rainer Hollmann	Science Coordinator		21/04/2016
Approval		CM SAF Steering Group		
Release	Martin Werscheck	Project Manager		

Distribution List

Internal Distribution	
Name	**No. Copies**
DWD Archive	1
CM SAF Team	1

External Distribution		
Company	**Name**	**No. Copies**
PUBLIC		1

Document Change Record

Issue/ Revision	Date	DCN No.	Changed Pages/Paragraphs
1.0	30/09/2012	SAF/CM/DWD/ATBD/SEV/CLD/1	Initial version, submitted for DRI7
1.1	25/02/2013	SAF/CM/DWD/ATBD/SEV/CLD/1.1	Revised version following DRI RIDs
2.0	28/04/2015	SAF/CM/DWD/ATBD/SEV/CLD/2.0	Updated version for CLAAS

Issue/ Revision	Date	DCN No.	Changed Pages/Paragraphs
			edition 2
2.1	22/06/2015	SAF/CM/DWD/ATBD/SEV/CLD/2.1	Revised version following PCR RIDs
2.2	20/04/2016	SAF/CM/DWD/ATBD/SEV/CLD/2.2	Revised version following algorithm adjustments made during feedback loop before final processing: These are described in sections 4.1.1, 4.1.2 and 4.3.1
2.3	17.06.2016	SAF/CM/DWD/ATBD/SEV/CLD/2.3	Update after DRR2.4 RIDs

Table of Contents

List of Figures

List of Tables

Figure 3-1: Overview of SEVIRI measurements record at CM SAF used as basis for cloud products. Short-term data gaps are shown enlarged for better visibility. Exact dates can be found in Table 3-4. 12

Figure 3-2: Time series of MSG-SEVIRI calibration slopes for the three solar channels as derived operationally by EUMETSAT (dashed) and from inter-calibration with Aqua-MODIS (symbols and solid line fits). The fit coefficients are indicated in the plots, with D – $D_{1/1/2000}$ being the number of days since 1 January 2000. 15

Figure 4-1: Effect of the CM SAF patch on the monthly mean cloud fraction in July 2009. Right column shows the bias (patch – original). Note that the change in non-coastal areas is mostly induced by reducing the segment size from 4 to 1. 18

Figure 4-2: Same as Figure 4-1 but for January 2009. 18

Figure 4-3: Spatial standard deviation (or variance) of the 0.6 µm and 0.8 µm radiances for one timeslot. The central plot in the bottom row displays the relative difference D. The lower right plot shows the binary mask D > 1: White represents *False*, red represents *True*. 19

Figure 5-1: Area seen by SEVIRI. Example is for cloud fractional cover. 22

Applicable documents

Reference	Title	Code
AD 1	CM SAF Product Requirements Document	SAF/CM/DWD/PRD/2.7

Reference documents

Reference	Title	Code
RD 1	Algorithm Theoretical Basis Document SAFNWC/MSG “Cloud Products” (CMa-PGE01 v3.2, CT-PGE02 v2.2 & CTTH-PGE03 v2.2)	SAF/NWC/CDOP/MFL/SCI/ATBD/01, Issue 3, Rev. 2, 15 Feb. 2012
RD 2	Algorithm Theoretical Basis Document Cloud physical products SEVIRI	SAF/CM/KNMI/ATBD/SEV/CPP/2.2
RD 3	MSG Level 1.5 Image Data Format Description	EUM/MSG/ICD/105 v7, 4 Dec. 2013

1 The EUMETSAT SAF on Climate Monitoring

The importance of climate monitoring with satellites was recognized in 2000 by EUMETSAT Member States when they amended the EUMETSAT Convention to affirm that the EUMETSAT mandate is also to "contribute to the operational monitoring of the climate and the detection of global climatic changes". Following this, EUMETSAT established within its Satellite Application Facility (SAF) network a dedicated centre, the SAF on Climate Monitoring (CM SAF, http://www.cmsaf.eu).

The consortium of CM SAF currently comprises the Deutscher Wetterdienst (DWD) as host institute, and the partners from the Royal Meteorological Institute of Belgium (RMIB), the Finnish Meteorological Institute (FMI), the Royal Meteorological Institute of the Netherlands (KNMI), the Swedish Meteorological and Hydrological Institute (SMHI), the Meteorological Service of Switzerland (MeteoSwiss), and the Meteorological Service of the United Kingdom (UK MetOffice). Since the beginning in 1999, the EUMETSAT Satellite Application Facility on Climate Monitoring (CM SAF) has developed and will continue to develop capabilities for a sustained generation and provision of Climate Data Records (CDRs) derived from operational meteorological satellites.

In particular the generation of long-term data sets is pursued. The ultimate aim is to make the resulting data sets suitable for the analysis of climate variability and potentially the detection of climate trends. CM SAF works in close collaboration with the EUMETSAT Central Facility and liaises with other satellite operators to advance the availability, quality and usability of Fundamental Climate Data Records (FCDRs) as defined by the Global Climate Observing System (GCOS). As a major task the CM SAF utilizes FCDRs to produce records of Essential Climate Variables (ECVs) as defined by GCOS. Thematically, the focus of CM SAF is on ECVs associated with the global energy and water cycle.

Another essential task of CM SAF is to produce data sets that can serve applications related to the new Global Framework of Climate Services initiated by the WMO World Climate Conference-3 in 2009. CM SAF is supporting climate services at national meteorological and hydrological services (NMHSs) with long-term data records but also with data sets produced close to real time that can be used to prepare monthly/annual updates of the state of the climate. Both types of products together allow for a consistent description of mean values, anomalies, variability and potential trends for the chosen ECVs. CM SAF ECV data sets also serve the improvement of climate models both at global and regional scale.

As an essential partner in the related international frameworks, in particular WMO SCOPE-CM (Sustained COordinated Processing of Environmental satellite data for Climate Monitoring), the CM SAF - together with the EUMETSAT Central Facility, assumes the role as main implementer of EUMETSAT's commitments in support to global climate monitoring. This is achieved through:

- Application of highest standards and guidelines as lined out by GCOS for the satellite data processing,
- Processing of satellite data within a true international collaboration benefiting from developments at international level and pollinating the partnership with own ideas and standards,
- Intensive validation and improvement of the CM SAF climate data records,
- Taking a major role in data set assessments performed by research organisations such as WCRP. This role provides the CM SAF with deep contacts to research organizations that form a substantial user group for the CM SAF CDRs,

- Maintaining and providing an operational and sustained infrastructure that can serve the community within the transition of mature CDR products from the research community into operational environments.

A catalogue of all available CM SAF products is accessible via the CM SAF webpage, www.cmsaf.eu/. Here, detailed information about product ordering, add-on tools, sample programs and documentation is provided.

2 Introduction

This CM SAF Algorithm Theoretical Basis Document (ATBD) provides information on the processing algorithms and chain implemented for the generation of the cloud products as part of the CLAAS-2 (CM SAF CLoud property dAtAset Using SEVIRI, edition 2). This dataset contains retrieved geophysical parameters from inter-calibrated measurements of the Spinning Enhanced Visible Infra-Red Imager (SEVIRI) mounted on the Meteosat Second Generation (MSG) satellites MSG-1, MSG-2, and MSG-3. The cloud property algorithms applied are the MSG v2012 software package by the NWCSAF (SAF for support to Nowcasting and Very Short Range Forecasting) used to derive cloud fraction and cloud top properties ([RD 1]; Derrien and Le Gléau, 2005), and the CPP (Cloud Physical Properties) algorithm ([RD 2]; Roebeling et al. 2006), which retrieves cloud-top thermodynamic phase, cloud optical thickness, cloud particle effective radius, and liquid/ice water path.

The document seamlessly describes all elements of the production of the final CLAAS-2 cloud products which are structured in the following three topics.

1. A description of the data sources and a summary of SEVIRI instrument characteristics are given, including a description of the inter-calibration applied to CLAAS-2 measurements.
2. A report on the derivation of the cloud products by applying CPP v5.2 and MSG v2012 algorithms. Note that significant parts of the MSG v2012 and CPP v5.2 algorithms have already been documented in the ATBDs [RD 1] and [RD 2], which will be referred to in this document when appropriate.
3. An elaboration on the production of the daily and monthly means (Level-3 data) based on the Level-2 products provided by CPP v5.2 and MSG v2012.

Basic accuracy requirements are defined in the product requirements document [AD 1].

The CLAAS-2 data set contains multiple cloud parameters derived from SEVIRI. The CM SAF release of CLAAS-2 contains the following cloud variables:

Fractional Cloud Cover [CM-21011, CFC, section 4.1]

Joint Cloud property histogram [CM-21021, JCH, section 4.2]

Cloud Top level [CM-21031, CTO, section4.3]

Cloud Phase [CM-21041, CPH, section 4.4]

Liquid Water Path [CM-21051, LWP, section4.5]

Ice Water Path [CM-21061, IWP, section 4.6]

.

3 Processing of measured SEVIRI radiances (Level-1.5)

3.1 The SEVIRI instrument

SEVIRI is a passive optical imaging radiometer with 12 spectral channels at visible and infrared wavebands. SEVIRI instruments are mounted on the geostationary MSG satellites and measure from 2004 onwards. MSG 1, MSG 2 and MSG 3 measurement images are to align to each other and centred at 0°/0° longitude/latitude. The region seen by a SEVIRI instrument is shown in Figure 5-1. It covers Africa, Europe, partly South America, the Atlantic Ocean and the Middle East. In Figure 3-1 the time-span of CLAAS-2 is displayed together with separation of available MSG 1, MSG 2 and MSG 3 measurements, also indicating gaps during the operation. All three SEVIRI instruments on MSG 1, MSG 2 and MSG 3 are identical in construction. Table 3-1 lists the main characteristics of the SEVIRI instrument. In the following the measurement principle is explained in the following.

An MSG satellite spins around its vertical axis with 100 rpm, the SEVIRI instrument uses this spin to scan the earth line-by-line in east-west direction. After each line, the scan mirror is moved on step in South-North direction and the next line is scanned. The acquisition time of one image is 12 minutes, together with onboard calibration and scan mirror retrace a nominal repeat cycle of 15 minutes is achieved.

For each of the 12 spectral channels three detectors acquire three lines of an image simultaneously. The HRV channel however has 9 detectors and 9 lines are obtained per revolution. In Table 3-2 SEVIRI’s channels and their characteristics can be found. After each scan a black body calibration is applied for the infrared channels as well as a measurement of the deep space radiance. The deep space radiance corresponds to zero input radiance and is subtracted from the measured signal. The black body calibration is undertaken by moving a black body into the telescope in the intermediate focal plane. The accuracy of SEVIRI was determined prior to the launch in space. The infrared channels measure brightness temperature with an accuracy of < 1 K for a target of 300 K while the bias for the VIS channels ranges from 0.08 to 0.52 W/(m² sr µm), for more details see Table 3-3.

After acquiring an image, the data are sent to the EUMETSAT ground segment where they are further processed into Level 1.5 data as described in the next section. After this processing step the images are ready to be disseminated to the user.

Table 3-1: SEVIRI instrument features.

line-by-line scanning radiometer
12 spectral channels 0.4 -13.4 µm, image every 15 min.
Scan duration 12 min.
blackbody calibration at every scan (15 min.)
spatial resolution: 3 km at sub-satellite point
radiometric bias: <1 K for IR and 1.5 – 11 W m^{-2} sr^{-1} mm^{-1} for VIS channels

Table 3-2: SEVIRI channel characteristics (source: EUMETSAT, 2010)

Channel ID	**Absorption Band / Channel Type**	**Nominal Centre Wavelength (µm)**	**Spectral Bandwidth (µm)**	**Dynamic Range**	**Spectral Bandwidth** As % of energy actually detected within spectral band
HRV	Visible High Resolution	Nominally 0.75	0.6 to 0.9	0 - 459 W/m2 sr m (scaled at centre frequency)	Precise spectral characteristics not critical
VIS 0.6	VNIR Core Imager	0.635	0.56 to 0.71	0 - 533 W/m2 sr m	98.0 %
VIS 0.8	VNIR Core Imager	0.81	0.74 to 0.88	0 - 357 W/m2 sr m	99.0 %
IR 1.6	VNIR Core Imager	1.64	1.50 to 1.78	0 - 75 W/m2 sr m	99.0 %
IR 3.9	IR / Window Core Imager	3.92	3.48 to 4.36	0 - 335 K	98.6 %
IR 6.2	Water Vapour Core Imager	6.25	5.35 to 7.15	0 - 300 K	99.0 %
IR 7.3	Water Vapour Pseudo-Sounding	7.35	6.85 to 7.85	0 - 300 K	98.0 %
IR 8.7	IR / Window Core Imager	8.70	8.30 to 9.10	0 - 300 K	98.0 %
IR 9.7	IR / Ozone Pseudo-Sounding	9.66	9.38 to 9.94	0 - 310 K	99.0 %
IR 10.8	IR / Window Core Imager	10.80	9.80 to 11.80	0 - 335 K	98.0 %
IR 12.0	IR / Window Core Imager	12.00	11.00 to 13.00	0 - 335 K	98.0 %
IR 13.4	IR / Carbon Dioxide Pseudo-Sounding	13.40	12.40 to 14.40	0 - 300 K	96.0 %

Table 3-3: SEVIRI channel noise budgets expressed in K for IR channels and W/(m² sr µm) as reported in Schmid (2000)

Channel (µm)	HRV	0,6	0,8	1,6	3,9	6,2	7,3	8,7	9,7	10,8	12	13,4
Noise	0,52	0,39	0,36	0,08	0,24	0,4	48	0,15	0,24	0,13	0,21	0,29
Spec.	1,07	0,53	0,49	0,25	0,35	0,75	0,75	0,28	1,5	0,25	0,37	1,8

3.2 The SEVIRI measurement record

The SEVIRI measurement record spans the time-period from 2004 onwards, measurements from the respective instrument on the satellite that was in operational mode was used. During the respective time-span, two operational changes took place, one from MSG 1 to MSG 2 in 2008 and from MSG 2 to MSG 3 in 2013.

In this edition of the dataset (CLAAS-2) SEVIRI's original temporal resolution is of 15 minutes is included, which is in contrast to CLAAS-1 for which only one slot per hour was considered.. The horizontal resolution of a SEVIRI image is 3 x 3 km² at nadir. CLAAS-2 covers the time-span Jan. 2004 to Dec. 2015, where MSG1 measurements were processed from 01/2004 – 04/2007, MSG 2 measurements from 04/2007 – 01/2013 and MSG 3 measurements from 01/2013 to 12/2015. Gaps of more than 24 hours in the time-series of the operational satellite were filled with MSG 1, or MSG2 measurements, respectively (Figure 3-1); exact dates with gaps and missing dates in the MSG record that could be filled with measurements of the backup satellite are listed in Table 3-4.

For the derivation of the cloud products the Level 1.5 SEVIRI data provided by EUMETSAT were used. Level 1 data is image data that was directly transferred to the EUMETSAT's ground segment. i.e. raw data before any modification has taken place. The Level 1.5 data record comprises image data that has already undergone certain modifications by EUMETSAT: it has been corrected for all unwanted radiometric and geometric effects, has been geolocated using a standardised projection, and has been calibrated and radiance-linearised.

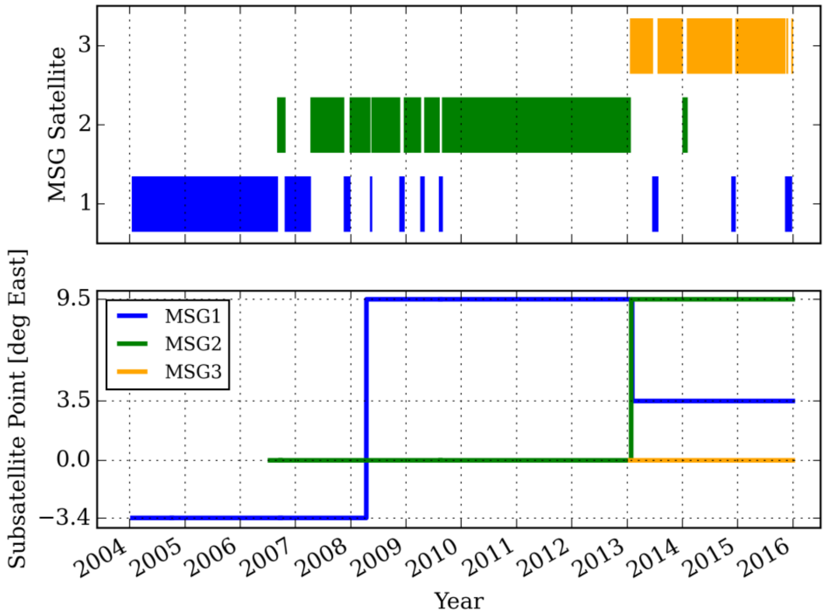

Figure 3-1: Overview of SEVIRI measurements record at CM SAF used as basis for cloud products. Short-term data gaps are shown enlarged for better visibility. Exact dates can be found in Table 3-4.

Some of the processing steps are described in the following: First, the raw data are projected onto the SEVIRI disk to form a geolocated image. Every image (except for HRV, which will not be described further, since its measurements are not used for CLAAS-2) consists of 3712 lines by 3712 columns. The space area of the Level 1.5 image is set to a predefined binary value, also the missing pixel will be replaced by this value. The sampling distance is defined to be exactly 3 km by 3 km at the sub-satellite point and the geolocation is centred at 0° latitude and 0° longitude where the centre is situated in the middle of the pixel with the line numbers (1856,1856).

The Level 1.5 images are delivered to the DWD in HRIT format. Each time slot or image package respectively consists of header information contained in a so-called prologue file and trailer information included in the epilogue file. All other files contain the image information of the channels. One image is divided into 8 segments, where each segment contains 464 image lines. The header files contain vital information concerning the image acquisition like status of the satellite or the instruments as well as the gain and offset coefficients. In the trailer files information about the geometric and radiometric quality as well as image production status is included.

The image data are stored in a 10 bit integer format, and therefore have been scaled. The user has to apply the gain and offset given in the header to receive the actual radiance values. Please note that EUMETSAT introduced a new radiance definition, changing from spectral radiance to effective radiance, in 2008 (see EUMETSAT, 2008). The whole SEVIRI Level 1.5 data archive was reprocessed by EUMETSAT and the new files were transferred to the DWD, so the complete CLAAS-2 dataset relies on the reprocessed Level 1.5 radiances.

Table 3-4: Gaps in SEVIRI measurement record of the prime MSG satellites. Gaps shorter than 1 day are not listed. Last column lists the backup satellites (if available) whose data is used to fill the gaps for CLAAS-2. Time period considered is Jan. 2004 to Dec. 2015.

Gaps in operational service of the prime MSG satellites		Prime satellite	Replacement
from	to		
05/10/2004	06/10/2004	MSG-1	no
24/09/2006	24/09/2006	MSG-1	no
25/09/2006	05/10/2006	MSG-1	MSG-2
04/12/2007	12/12/2007	MSG-2	MSG-1
14/05/2008	16/05/2008	MSG-2	MSG-1
02/12/2008	08/12/2008	MSG-2	MSG-1
18/04/2009	23/04/2009	MSG-2	MSG-1
16/08/2009	16/08/2009	MSG-2	no
17/08/2009	21/08/2009	MSG-2	MSG-1
02/07/2013	09/07/2013	MSG-3	MSG-1
15/01/2014	21/01/2014	MSG-3	MSG-2
03/12/2014	08/12/2014	MSG-3	MSG-1
16/11/2015	18/11/2015	MSG-3	MSG-1
09/12/2015	14/12/2015	MSG-3	MSG-1

3.3 Applied SEVIRI solar channel calibration description

SEVIRI does not carry an on-board calibration device for the solar channels. Therefore, EUMETSAT operates a vicarious calibration system using Earth targets (desert and ocean) as reference. Analyses by Doelling et al. (2004) and Ham and Sohn (2010) revealed that the resulting visible channel nominal calibration, provided in the SEVIRI Level-1.5 data files, has a considerable offset with respect to MODIS, which is thought to be a well-calibrated reference instrument. Meirink et al. (2013) extended these previous analyses to the NIR channels and to longer time periods. They used collocated, ray-matched, atmosphere-corrected, near-nadir SEVIRI and Aqua-MODIS reflectances to derive inter-calibration slopes, i.e. multiplicative factors to be applied to SEVIRI nominal reflectance in order to match the MODIS measurements. Recently, this calibration work was extended to cover the full CLAAS-2 time window of 2004 to 2014, including all three SEVIRI instruments that have been active. The same method was applied as described in Meirink et al. (2013) but now using MODIS Collection 6 instead of Collection 5 Level-1b data as a reference. Results are shown in Figure 3-2.The operational MSG-SEVIRI calibration is offset relative to Aqua-MODIS by about -8%, -6% (but -4% for MSG-3), and +3%, for channels 1, 2, and 3, respectively. Furthermore, even if the SEVIRI calibration turns out to be quite stable over time, there are significant trends. For CLAAS-2 processing the calibration slopes shown by the solid lines in Figure 3-2 will be used..

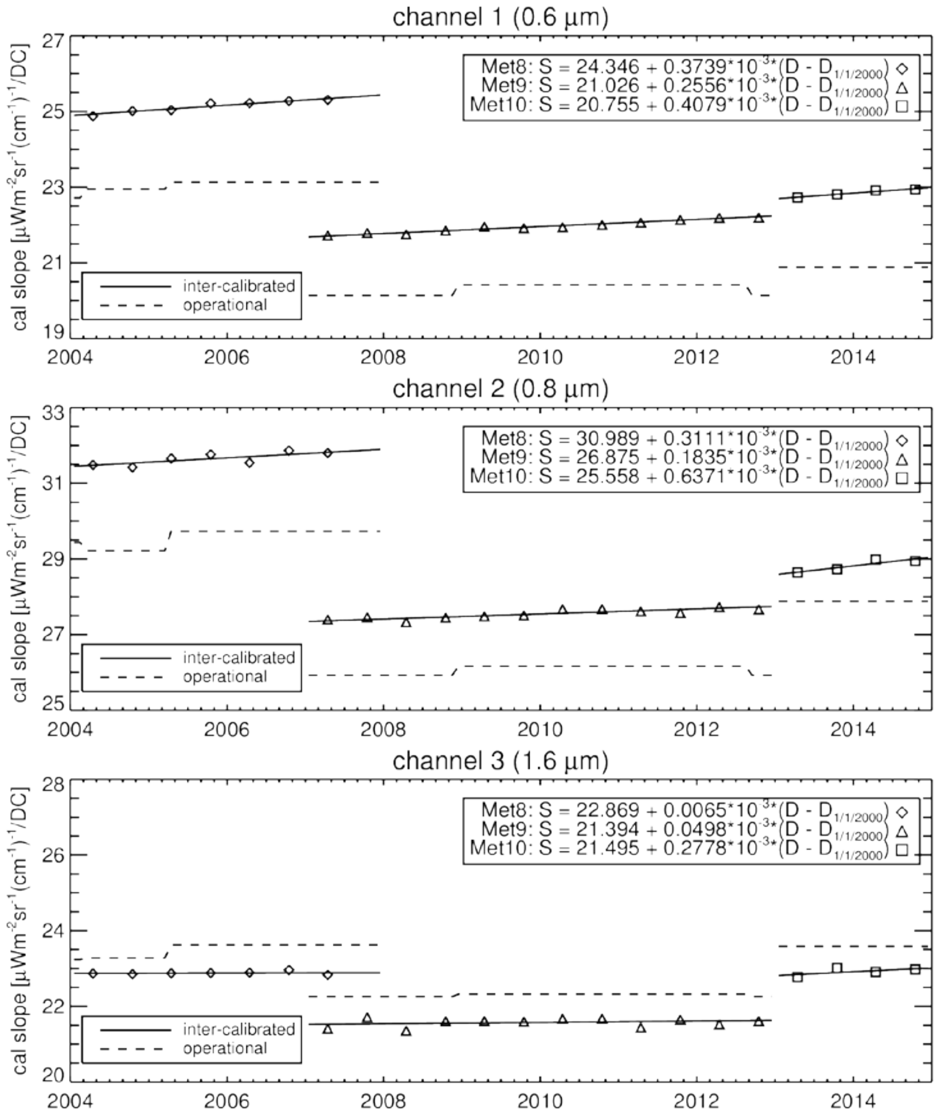

Figure 3-2: Time series of MSG-SEVIRI calibration slopes for the three solar channels as derived operationally by EUMETSAT (dashed) and from inter-calibration with Aqua-MODIS (symbols and solid line fits). The fit coefficients are indicated in the plots, with D – $D_{1/1/2000}$ being the number of days since 1 January 2000.

4 Retrieval of pixel-based cloud properties (Level-2)

This section provides information on the processing of MSG v2012 and CPP v5.2 to retrieve cloud parameters from inter-calibrated SEVIRI measurements. Each parameter is briefly introduced in the following with the respective detailed ATBD being referred to.

4.1 Fractional Cloud Cover [CM-21011, CFC]

This product is derived directly from results of a cloud screening or cloud masking method. The cloud mask comprises 6 categories: Cloud filled, cloud-free, cloud contaminated and non-processed, snow/ice contaminated, undefined. The cloud fractional cover is defined as the fraction of cloudy pixels per grid cell compared to the total number of analyzed pixels in the grid cell. Pixels are counted as cloudy if they belong to the classes cloud filled or cloud contaminated. Fractional cloud cover is expressed in percent. The cloud screening and cloud masking is performed using a custom modified version of the NWC SAF MSG v2012 algorithm. The basic algorithm is described in more detail in [RD 1], the custom modifications are explained in the following subsections.

4.1.1 Reducing the Segment Size

In the default SAFNWC-MSGv2012 cloud masking algorithm, computation time is reduced by computing one threshold for segments of 4x4 SEVIRI pixels. In order to exploit the full potential of the SEVIRI sensor, we reduce the segment size to one, so that individual thresholds are computed for each pixel. The increase in computation time is compensated by a higher degree of parallelization.

4.1.2 Reducing Coastal Cloud Mask Artifacts

We discovered systematically lower cloud fraction along the North Sea and Atlantic coasts in northern Europe (see Figure 4-1, left column). In [RD 1], the developers describe cloud mask false alarms near coasts caused by so called variance tests. For each pixel in a certain channel at wavelength λ, the spatial standard deviation, VAR_{λ} of the radiance is computed among the 8 surrounding pixels and the pixel itself. The pixel is set to cloudy, if the standard deviation exceeds a certain predefined threshold. Variance tests are skipped, if there is a coastline within the 3x3 pixel box. In order to reduce these artifacts, SAFNWC implemented a reclassification algorithm removing isolated cloud clusters near coasts, which were detected by a variance test. As it turned out, the reclassification algorithm is removing too many clouds leading to the observed local cloud fraction minima near coasts.

Instead of just relaxing the reclassification criterion, we tried to find a solution which is independent of the coast information. For this purpose we determined the SEVIRI channels responsible for the false alarms, i.e. the channels with increased spatial variance near coasts. The main contributions come from the 0.8 μm visible channel and the thermal 10.8 μm infrared channel. We assume that the increased variance in the visible channel might be caused by the sea floor shining through towards the coastline. This gradient would then lead to an increased variance over the coastal waters. In case of the infrared channel, there might be a relation to the shallow coastal waters warming (in summer) and cooling (in winter) faster than deeper regions. Such a temperature gradient would also manifest in an increased variance over the coastal waters. Of course, spatial variance can also be caused by real clouds, so the challenge is to find a criterion separating cloud induced variance from non-cloud induced variance.

We found the relative difference

$$D = (VAR_{0.8} - VAR_{0.6})/VAR_{0.6}$$

to be a good indicator of non-cloud induced variance: As one can see in Figure 4-3, both channels share the same features, except for cloud-free coastal waters, where $VAR_{0.8}$ is significantly larger than $VAR_{0.6}$. Thus we disabled any variance test in SAFNWC-MSG, if $D > 1$ and the solar zenith angle < 88 degrees. If the solar zenith angle becomes too large, the difference between $VAR_{0.6}$ and $VAR_{0.8}$ vanishes, making the criterion unusable. However, it turned out, that some artifacts still remain, so that we finally implemented a hybrid approach of the above criterion together with a moderate, range-extended sea-only version of the reclassification algorithm by SAFNWC.
As one can see in the center column of Figure 4-1, the hybrid approach works fine in (northern hemisphere) summer, but things become more complicated in winter when coastal false alarms from infrared channels increase significantly (Figure 4-2). At daytime, they are suppressed by the hybrid approach, but since it depends on visible channels, it is not applicable at night, leading to a higher cloud fraction over coastal waters in winter nights. Unfortunately we did not find a pair of infrared channels which could be used similarly to predict coastal false alarms. However, the obtained results are still an improvement compared to the original SAFNWC-MSG version.

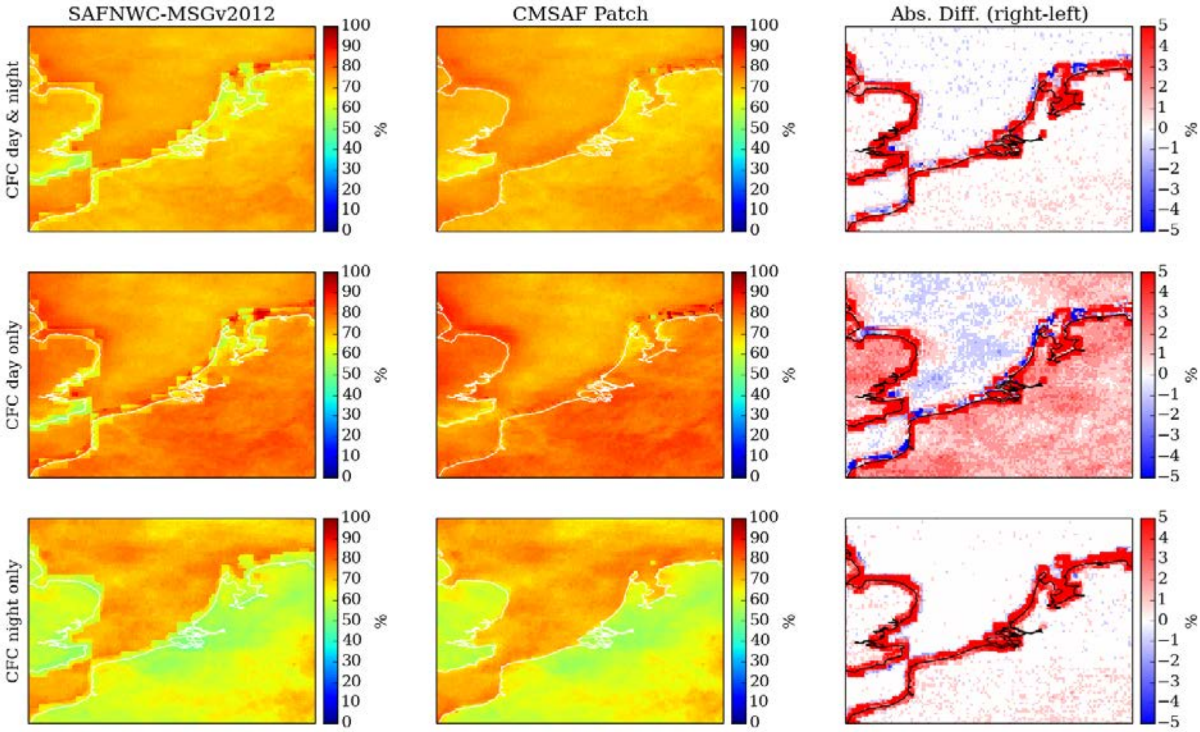

Figure 4-1: Effect of the CM SAF patch on the monthly mean cloud fraction in July 2009. Right column shows the bias (patch – original). Note that the change in non-coastal areas is mostly induced by reducing the segment size from 4 to 1.

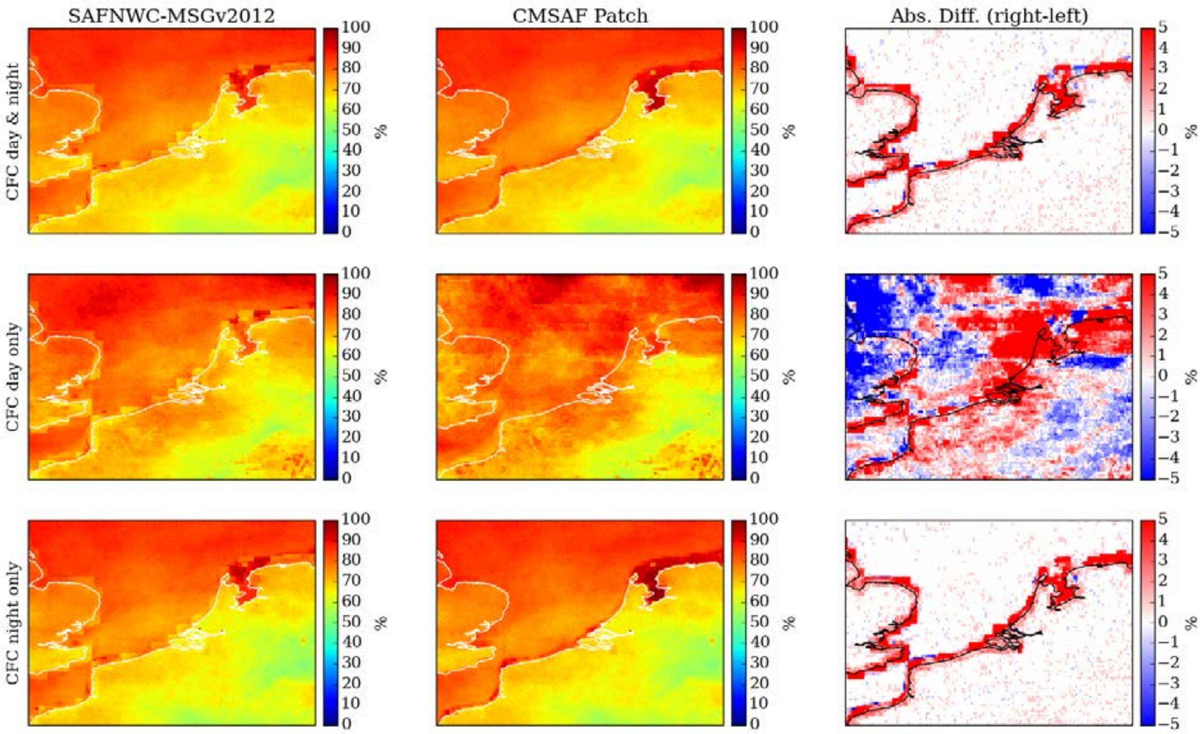

Figure 4-2: Same as Figure 4-1 but for January 2009.

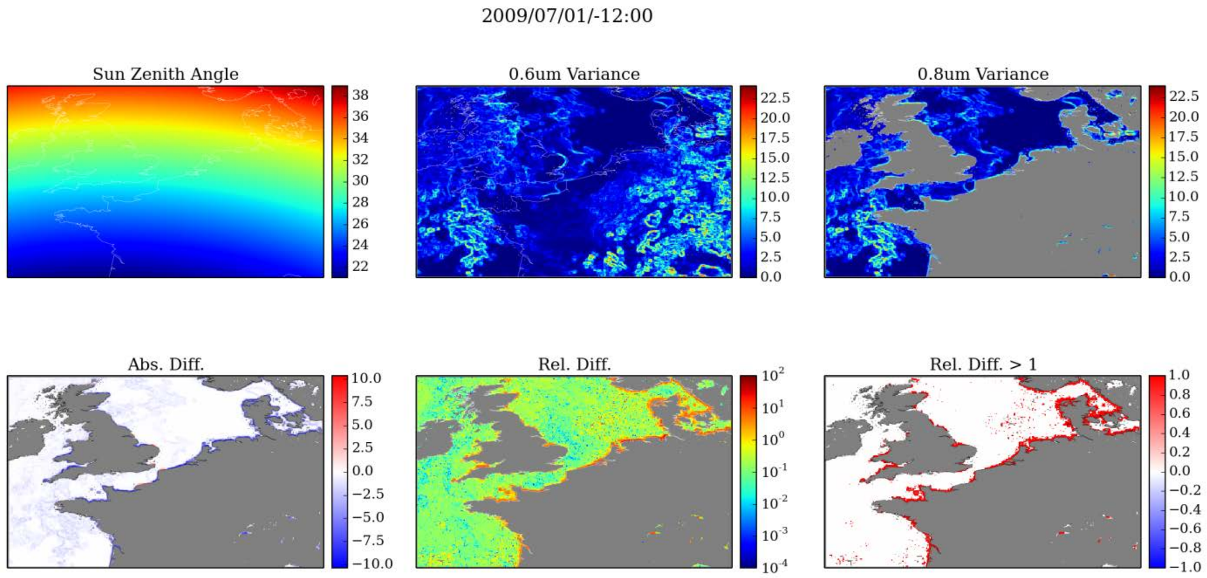

Figure 4-3: Spatial standard deviation (or variance) of the 0.6 µm and 0.8 µm radiances for one timeslot. The central plot in the bottom row displays the relative difference D. The lower right plot shows the binary mask D > 1: White represents *False*, red represents *True*.

4.2 Joint Cloud property Histogram [CM-21021, JCH]

The JCH product is a combined histogram of CTP (see Section4.3), COT (see Sections 4.5 and 4.6), and CPH (see Section 4.4), covering the solution space of these parameters. This three-dimensional histogram gives the absolute numbers of occurrences for specific COT-CTP-CPH combinations defined by specific bins, which can be found in section 5.2.2.

4.3 Cloud Top level [CM-21031, CTO]

Three versions of the CM SAF Cloud Top product exist: 1. Cloud Top Temperature (CTT), expressed in Kelvin; 2. Cloud Top Height (CTH), expressed as altitude above sea level (m); 3. Cloud Top Pressure (CTP), expressed in pressure co-ordinates (hPa). Cloud top products are retrieved with the following method.

In a first step, cloudy pixels are separated into three classes depending on cloud type or its opacity respectively: 1. very low, low or medium thick as well as middle level clouds; 2. high opaque clouds; 3. high semi-transparent clouds.

Using RTTOV (http://research.metoffice.gov.uk/research/interproj/nwpsaf/rtm/) the corresponding radiances and brightness temperatures for overcast and clear sky are simulated for each pixel, with vertical profiles of temperature and humidity analysis from ERA-Interim (Dee et al., 2012) as ancillary input. The SEVIRI channels used are: 6.2, 7.3, 13.4 10.8, 12.0 µm.

For very low, low or medium thick clouds as well as opaque clouds the cloud top pressure is retrieved as the best fit between the simulated and the measured 10.8µm brightness temperatures. Also the possibility of a low level thermal inversion is taken into account with the help of the ERA-Interim temperature profile at the respective pixel. In that case the very low, low or medium clouds are assumed to form at the inversion level, while they can also rise above that level if their brightness temperatures are colder than the air temperature below the thermal inversion minus an offset, that depends on the type of the inversion (dry air above the inversion level or not). This dependence results from the question if the inversion follows an try or wet adiabatic curve.

In case of semitransparent clouds the H2O/IRW intercept method is used, in which the radiances in each sounding channels is used together with the radiance in the window channel and each radiance pair is compared to simulated radiances of opaque clouds. When cloud top pressure cannot be obtained from at least two sounding channels, the radiance rationing method is used, in which the ratio of radiances from 2 channels is compared to simulated radiances at clear sky conditions for a fixed temperature profile.. For the latter a linear relationship of radiance between 2 spectral bands is assumed, but a curve for a window and a sounding channel. For opaque clouds this technique is always applied as preceding test, in order to remove any pixels that are semitransparent but where in fact falsely labeled as opaque by the cloud type test.

The retrieval algorithms are part of the NWC SAF MSG v2012 package, details can be found in [RD 1]. These algorithms were applied with a patch as described below.

4.3.1 Extremely High Cloud Top Temperature

Extremely high cloud top temperatures > 340K were noticed in the level 2 data. Further investigation revealed that these were actually very low retrieved temperatures that fell below the lower scaling limit in the output files, and were then rendered as high temperatures. After contacting SAFNWC, a patch was provided to fix this problem. It was caused by a software bug in a spatial smoothing module.

4.4 Cloud Phase [CM-21041, CPH]

The cloud phase product is meant to represent the thermodynamic phase of the particles near the cloud top. The cloud-top phase retrieval is based on a number of threshold tests using SEVIRI channels IR_6.2, IR_8.7, IR_10.8, IR_12.0, and IR_13.4. Some of the tests involve clear and cloudy-overcast radiances, which are calculated using RTTOV. The algorithm is run for cloudy pixels and initially yields one of the following cloud types: liquid, supercooled, opaque ice, cirrus, overlap, and overshooting. These are then further condensed to liquid (former two) and ice (latter four) phase. Details on the algorithm can be found in [RD 2].

4.5 Liquid Water Path [CM-21051, LWP]

For pixels to which the liquid phase has been assigned, liquid water path (LWP) is derived from the cloud optical thickness (COT or τ) and particle effective radius (REF or r_e). The τ - r_e retrieval scheme, developed at KNMI, uses a pair of satellite radiances at wavelengths in the non-absorbing (for clouds) visible and the moderately absorbing solar infrared part of the spectrum, following methods introduced by, e.g., Nakajima and King (1990). The observed radiances are iteratively matched with values simulated with the Doubling Adding KNMI (DAK, De Haan et al., 1987) radiative transfer model and stored in lookup tables (LUTs), yielding τ between 0.1 and 100 and r_e between 3 and 34 µm. Scattering properties were calculated with Mie theory for spherical droplets. The SEVIRI channels VIS_0.6 and IR_1.6

are used for the retrieval. Maximum solar and satellite zenith angles for which retrievals are peformed are 84 degrees.

Liquid water path is then computed from the retrieved τ and r_e values by (Stephens, 1978): LWP = 2/3 ρ_l τ r_e, in which ρ_l represents the density of liquid water (1000 kg m-3). More details on the retrieval scheme can be found in [RD 2].

In addition to LWP, COT and REF are provided as additional layers in the product files. Moreover, uncertainty estimates of these parameters are given.

4.6 Ice Water Path [CM-21061, IWP]

For pixels to which the ice phase has been assigned, ice water path (IWP) is retrieved in the same way as LWP described in Section4.5. Here, the scattering properties were calculated with a raytracing code (Hess et al. 1998) using the geometric optics approximation for randomly oriented, roughened, hexagonal ice crystals with effective radii between 5 and 80 µm. IWP is then computed with the same formula as LWP but with the density of ice (930 kg m-3). More details on the retrieval scheme can be found in [RD 2].

As for LWP, COT and REF are provided as additional layers in the product files, and error estimates of these parameters are given.

5 Generation of daily and monthly means, and histograms (Level-3)

In addition to the Level 2 pixel-level products, which are on native SEVIRI projection and resolution, CLAAS-2 also contains Level 3 products of various parameters and parameter combinations. The pixel level retrieval results of the Level 2 algorithm software of CPP v5.2 and MSG v2012 are input to the L2/L3 processing. The L3 outputs produced are fields of daily and monthly averages (and histograms) with specification defined in [AD 1]. These specifications are summarized in section 5.1. The covered geographic area is shown in Figure 5-1. The Level 2 data pixels are projected onto a regular latitude/longitude grid with a resolution of (0.05°)² and both collected in daily histograms as well as averaged to daily means. An exception are the JCH for which the lat/lon resolution is (0.25°)². The daily means/histograms and then further processed to monthly means/histograms with each daily data being weighted equally.

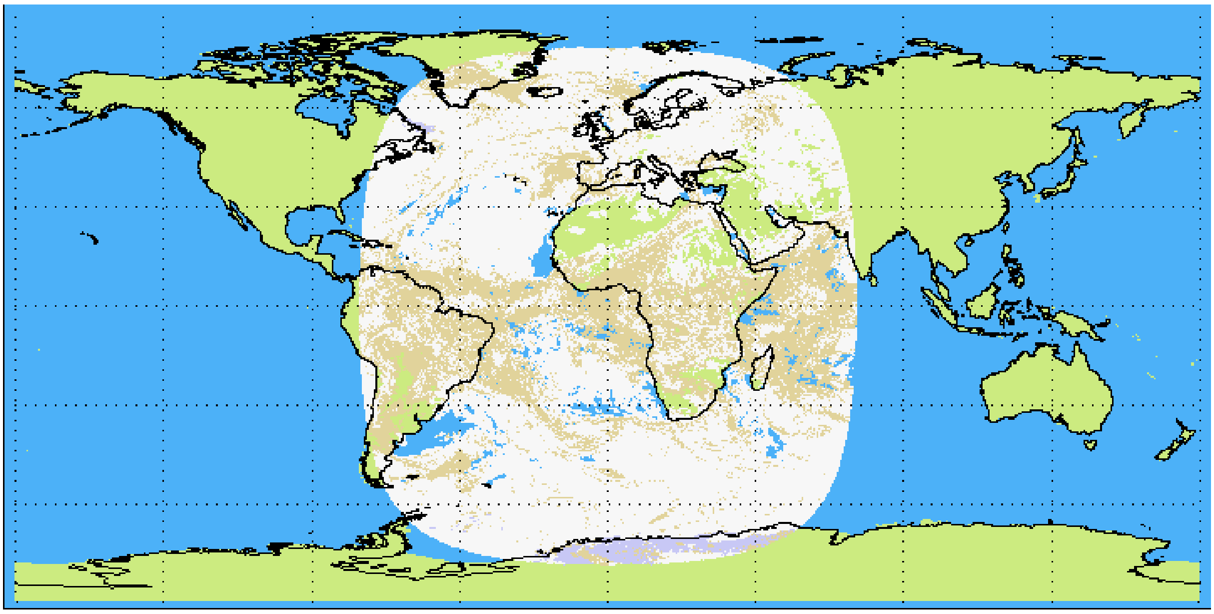

Figure 5-1: Area seen by SEVIRI. Example is for cloud fractional cover.

5.1 Definition of product specifications

The CLAAS-2 cloud data set provides a number of cloud parameters on the area indicated in Figure 5-1. Instantaneous retrievals with a temporal resolution of 15 minutes at original spatial resolution are used to derive the spatio-temporally collected data sets. The products are available as daily mean as well as monthly means/histograms on a regular latitude/longitude grid with a spatial resolution of 0.05° × 0.05° degrees. Also, monthly mean diurnal cycles are generated consisting of 24 time-steps with a spatial resolution of 0.25° × 0.25° degrees. The data of each of the 24 time steps is calculated by averaging all 4 time slots of a particular hour (‘00,’15,’30,’45) over all days of a month.

Acknowledging the different observation capabilities during night and during day and also taking into account existing diurnal variations in cloudiness, a further separation of results in daytime and night-time portions has also been done (for fractional cloud cover and cloud phase). Here, all observations made under twilight conditions (solar zenith angle between 75° and 95°) have been excluded in order to avoid being affected by specific cloud detection problems occurring in the twilight zone.

In addition to the mean values, histograms are provided on monthly time scales. The Joint Cloud property Histograms are two-dimensional histograms of COT and CTP are composed with a spatial resolution of 0.25° x 0.25° degrees. (See Section 5.3.2 for more technical details). For CTP, COT, REF, CWP one-dimensional histograms are constructed on a monthly basis with a spatial resolution of 0.05° × 0.05° degrees, each separately for liquid and ice clouds (see Sections 5.3.3, 5.3.4, 5.3.6 and 5.3.7 for more technical details.).

5.2 Calculation of Level 3 products

For the daily averages/histograms all data fields with original SEVIRI pixel size and in 15 minutes resolution are temporally averaged and collected. Here, all values are considered equally valid, thus no weighting is applied. In contrast to CLAAS-1, monthly means/histograms are generated from daily data.

It is important to note that different quality checks are applied for filtering valid numbers for each parameter. This is motivated by the fact that not in all cases where a cloud mask is available all cloud retrieval results of CPH, CTO, COT, REF, LWP and IWP are available.

5.2.1 Fractional Cloud Cover [CFC]

The daily mean fractional cloud cover is calculated from the aggregation of the instances of the binary cloud mask information as follows:

$$CFC(i,j) = \frac{N(i,j)_{Cloudy}}{N(i,j)_{Cloudy} + N(i,j)_{Clear}} \qquad (1)$$

with i and j being the indices of the original field projection, $N(i,j)_{Cloudy}$ the number of cloudy cases and $N(i,j)_{Clear}$ the number of clear cases. Acknowledging the different cloud detection capability during day and night time, an additional separation is done leading to $CFC(i,j)_{Night}$ and $CFC(i,j)_{Day}$, separate day time and night time averages. Here, the solar zenith angle of ≤75° and ≥95° are used to define day and night, respectively. Cases with solar zenith angles between 75° and 95°are included the nominal daily mean but excluded when collecting data for day-only and night-only averages. The monthly mean cloud fractional cover is calculated as mean over the daily means with each day being weighted equally.

5.2.2 Joint Cloud property Histogram [JCH]

Differing from CFC, CPH, LWP and IWP product derivation, the JCH does not include a classical mean of a specific cloud property but covers the solution space for the 3 cloud parameters: COT, CTP and CPH. Hence, the JCH product is only available for daytime observations, defined as observations with solar zenith angle lower than 75°. This product is described in a five-dimensional field $JCH(i, j, t, p, ph)$. Indices i and j refer to location space, while t and p being the indices for specific bins of the range of occurring COT and CTP values, and ph denotes the cloud phase.

Each specific field entry contains the absolute number cloud pixels with phase ph falling into the COT bin t and the CTP bin p being. The following values bordering the bins of COT and CTP (given in hPa) have been defined:

COT:{ 0, 0.3, 0.6, 1.3, 2.2, 3.6, 5.8, 9.4, 15, 23, 41, 60, 80, 100, inf} and

CTP:{ 1, 90, 180, 245, 310, 375, 440, 500, 560, 620, 680, 740, 800, 875, 950, 1100} [hPa].

These histograms are calculated for liquid and ice clouds separately, thus:

$$JCH(i,j,t,p)_{ice} = N(i,j)_{COT\varepsilon COTbin;CTP\varepsilon CTPbin;CPH=ice} \quad (2)$$

and

$$JCH(i,j,t,p)_{liquid} = N(i,j)_{COT\varepsilon COTbin;CTP\varepsilon CTPbin;CPH=liquid} \quad (3)$$

and merged into one field (JCH(I,j,t,p,ph)).

5.2.3 Cloud Top Level [CTO]

The CTO product contains daily means for CTH, CTP, and CTT. For these parameters all valid entries of the original fields are aggregated and then weighted by the number of used entries.

$$< x(i,j) >= \frac{1}{N(i,j)_{Cloudy}} \sum_{k=1}^{N(i,j)_{Cloudy}} x_k(i,j) \quad (4)$$

with $x(i,j)$ being a general expression for CTH, CTP and CTT at a specific original grid cell.

After temporal averaging, the fields are remapped to the final resolution as described in section 5.1.

For CTP, an alternative way of averaging is followed and additionally calculated and provided as geometrical mean where the variables are averaged in logarithm space:

$$< ctp(i,j) >_{\ln} = \exp(\frac{1}{N(i,j)_{Cloudy}} \sum_{k=1}^{N(i,j)_{Cloudy}} \ln(ctp_k(i,j))) \quad (5)$$

Geometrical mean is added to keep consistency between CTH and CTP. CTP depends logarithmically on CTH, so if CTH is averaged linearly, CTP has to be averaged logarithmically to preserve the relation.

The monthly mean cloud top level parameters are calculated as mean over the daily means with each day being weighted equally.

One-dimensional monthly histograms are generated for CTP on the same spatial resolution, but only on monthly basis. The CTP bin borders for these histograms are:

CTP:{ 1, 90, 180, 245, 310, 375, 440, 500, 560, 620, 680, 740, 800, 875, 950, 1100} [hPa].

5.2.4 Cloud Phase [CPH]

Similarly to CFC, the daily and averages of CPH are calculated by temporal averaging of retrieval results on original pixel basis and subsequent remapping. CPH is expressed as fraction of liquid water clouds by calculating the ratio of number of detected liquid clouds $N(i,j)_{Cloudy}$ with respect to the total number detected clouds $N(i,j)_{Cloudy}$:

$$CPH(i,j) = \frac{N(i,j)_{liquid}}{N(i,j)_{Cloudy}} \quad (6)$$

The monthly mean CPH is calculated as mean over the daily means with each day being weighted equally.

5.2.5 Liquid Water Path [LWP]

Daily mean LWP is calculated for each grid cell <LWP(i,j)> as given in Equation (4). Liquid clouds COT and REF are aggregated in the same way, and provided as additional data layers. Furthermore, for COT a logarithmic average is included, which is more consistent with the cloud radiative effect.

In addition to the in-cloud averages, all-sky LWP and COT are calculated by a weighting of the LWP with the CFC including cloud-free and ice-cloud pixels as zeroes in the averaging.

The in-cloud and all-sky monthly mean LWP (as well as the monthly mean of COT and REF of liquid clouds) are calculated as mean over the daily means with each day being weighted equally.

One-dimensional histograms are generated for LWP (and for COT and REF of liquid clouds) on the same spatial resolution, but only on monthly basis. Practically, these histograms are included in the liquid dimension of the CWP, COT and REF histograms with the following bin borders:

CWP: {0, 5, 10, 20, 35, 50, 75, 100, 150, 200, 300, 500, 1000, 2000, inf} [g/m^2]

COT: {0.0, 0.3, 0.6, 1.3, 2.2, 3.6, 5.8, 9.4, 15.0, 23.0, 41.0, 60.0, 80.0, 100, inf}

REF: {3, 6, 9, 12, 15, 20, 25, 30, 40, 60, 80} [µm].

5.2.6 Ice Water Path [IWP]

Daily mean IWP, as well as the ice cloud COT and REF, are calculated in exactly the same way as LWP. This includes the computation of all-sky IWP and COT by including cloud-free and liquid-cloud pixels as zeroes in the averaging.

The in-cloud and all-sky monthly mean IWP (as well as the monthly mean of COT and REF of ice clouds) are calculated as mean over the daily means with each day being weighted equally.

One-dimensional histograms are generated for IWP (and for COT and REF of ice clouds) on the same spatial resolution, but only on monthly basis. Practically, these histograms are included in the ice dimension of the CWP, COT and REF histograms with the following bin borders:

CWP: {0, 5, 10, 20, 35, 50, 75, 100, 150, 200, 300, 500, 1000, 2000, inf} [g/m^2]

COT: {0.0, 0.3, 0.6, 1.3, 2.2, 3.6, 5.8, 9.4, 15.0, 23.0, 41.0, 60.0, 80.0, 100, inf}

REF: {3, 6, 9, 12, 15, 20, 25, 30, 40, 60, 80} [µm].

5.3 Additional statistical parameters

In addition to the daily and monthly mean values, the standard deviations s over all valid and used values is calculated for CFC, CPH, CTO, LWP and IWP for each grid box with

$$s(x(i,j)) = (< x^2(i,j) > - < x(i,j) >^2)^{0.5}$$

For cloud microphysical properties, CWP, COT and REF, the retrieval defines an uncertainty which is also presented in the daily mean and monthly mean as well as its standard deviation.

5.4 Monthly mean diurnal cycles

To facilitate the assessment of monthly mean diurnal cycle for the user not only daily and monthly means are created but also monthly mean diurnal cycles from the quantities CFC, CTO, COT, LWP, IWP and CPH. For a monthly mean diurnal cycle, all fields of a specific slot are considered and averaged hour wise, the result is a file with 24 fields. Each field contains the monthly average of all input fields of a specific hour (including 4 time slots per hours: ’00, ’15, ’30, ‘45). Please note that the time axis refers to UTC; for a depiction in local time the pixel will have to be sorted with respect to the time zones.

6 References

CDO, 2009: CDO User's Guide. (Uwe Schulzweida, Luis Kornblueh – MPI for Meteorology Ralf Quast – Brockmann Consult) Available at: http://www.mpimet.mpg.de/fileadmin/software/cdo/cdo.pdf

De Haan, J. F., P. Bosma, and J. W. Hovenier, 1987: The adding method for multiple scattering calculations of polarized light, Astron. Astrophys., 183, 371-391.

Dee, D. P., Uppala, S. M., Simmons, A. J., Berrisford, P., Poli, P., Kobayashi, S., Andrae, U., Balmaseda, M. A., Balsamo, G., Bauer, P., Bechtold, P., Beljaars, A. C. M., van de Berg, L., Bidlot, J., Bormann, N., Delsol, C., Dragani, R., Fuentes, M., Geer, A. J., Haimberger, L., Healy, S. B., Hersbach, H., Hólm, E. V., Isaksen, L., Kållberg, P., Köhler, M., Matricardi, M., McNally, A. P., Monge-Sanz, B. M., Morcrette, J.-J., Park, B.-K., Peubey, C., de Rosnay, P., Tavolato, C., Thépaut, J.-N. and Vitart, F. (2011), The ERA-Interim reanalysis: configuration and performance of the data assimilation system. Q.J.R. Meteorol. Soc., 137: 553–597. doi: 10.1002/qj.828

Derrien, M. and H. Le Gléau, 2005, MSG/SEVIRI cloud mask and type from SAFNWC, International Journal of Remote Sensing, **26**, No. 21, 10 November 2005, 4707–4732.

Doelling, D. R., L. Nguyen, and P. Minnis, 2004: Calibration comparisons between SEVIRI, MODIS, and GOES data. In Proceedings of the 2004 EUMETSAT Meteorological Satellite Conference, Prague, Czech Republic. EUMETSAT.

EUMETSAT, 2010: MSG Level 1.5 Image Data Format Description, EUM/MSG/ICD/105 v6.

EUMETSAT, 2007: A Planned Change to the MSG Level 1.5 Image Product Radiance Definition, EUM/OPS-MSG/TEN/06/0519.

Ham, S.-H. and B. J. Sohn, 2010: Assessment of the calibration performance of satellite visible channels using cloud targets: application to Meteosat-8/9 and MTSAT-1R. Atmospheric Chemistry and Physics, 10(22), 11131–11149.

Hess, M., R. B. A. Koelemeijer, and P. Stammes, 1998: Scattering matrices of imperfect hexagonal crystals. *J. Quant. Spectrosc. Ra.*, **60**, 301–308.

Meirink, J.F., R.A. Roebeling and P. Stammes, 2013: Inter-calibration of polar imager solar channels using SEVIRI, Atm. Meas. Tech., 6, 2495-2508, doi:10.5194/amt-6-2495-2013.

Nakajima, T., and M. D. King, 1990: Determination of the Optical Thickness and Effective Particle Radius of Clouds from Reflected Solar Radiation Measurements. Part 1: Theory. J. Atmos. Sci ., 47, 1878-1893.

Roebeling, R.A., A.J. Feijt and P. Stammes, 2006: Cloud property retrievals for climate monitoring: implications of differences between SEVIRI on METEOSAT-8 and AVHRR on NOAA-17, J. Geophys. Res., **111**, D20210, doi:10.1029/2005JD006990.

Schmid, J., 2000: "The SEVIRI instrument." Proceedings of the 2000 EUMETSAT Meteorological Satellite Data User's Conference, Bologna, Italy, 29 May–2 June 2000.

Stephens, G. L., 1978: Radiation profiles in extended water clouds: II. Parameterization schemes. J. Atmos. Sci., **35**, 2123-2132.

7 Glossary

ATBD	Algorithm Theoretical Basis Document
AVHRR	Advanced Very High Resolution Radiometer
CDO	Climate Data Operators
CDOP	Continuous Development and Operations Phase
CFC	Fractional Cloud Cover
CLARA-A1	CM SAF cLoud, Albedo and Radiation products, AVHRR-based,
CLAAS	CM SAF CLoud property dAtaset Using SEVIRI
CM SAF	Satellite Application Facility on Climate Monitoring
CPH	Cloud Phase
COT	Cloud Optical Thickness
CTH	Cloud Top Height
CTO	Cloud Top product
CTP	Cloud Top Pressure
CTT	Cloud Top Temperature
CPP	Cloud Physical Properties
DRI	Delivery Readiness Inspection
DWD	Deutscher Wetterdienst (German MetService)
ECMWF	European Centre for Medium-Range Forecasts
ECV	Essential Climate Variable
ERA-Interim	Second ECMWF Re-Analysis dataset
EUMETSAT	European Organisation for the Exploitation of Meteorological
FCDR	Fundamental Climate Data Record
GCOS	Global Climate Observing System
IRW	Infrared window
ISCCP	International Satellite Cloud Climatology Project
IWP	Ice Water Path
JCH	Joint Cloud properties Histogram
KNMI	Koninklijk Nederlands Meteorologisch Instituut (Dutch MetService)
LWP	Liquid Water Path
MODIS	Moderate Resolution Imaging Spectroradiometer
MSG	Meteosat Second Generation
NOAA	National Oceanic & Atmospheric Administration

NWC SAF	SAF on Nowcasting and Very Short Range Forecasting
NWP	Numerical Weather Prediction
PRD	Product Requirement Document
PUM	Product User Manual
SEVIRI	Spinning Enhanced Visible and InfraRed Imager
SAF	Satellite Application Facility
SMHI	Swedish Meteorological and Hydrological Institute